International Journal of GEOMATE, June., 2021, Vol.20, Issue 82, pp.15-21
ISSN: 2186-2982 (P), 2186-2990 (O), Japan, DOI: https://doi.org/10.21660/2021.82.Gx185
Geotechnique, Construction Materials and Environment

ESTIMATION OF SUBSURFACE STRUCTURES AND GROUND MOTION CHARACTERISTICS IN THE AREAS DAMAGED IN THE 2016 CENTRAL TOTTORI PREFECTURE EARTHQUAKE IN JAPAN

*Isamu Nishimura[1], Tatsuya Noguchi[1] and Takao Kagawa[1]

[1]Graduate school of Engineering, Tottori University, Japan

*Corresponding Author, Received: 30 Nov. 2020, Revised: 10 Feb. 2021, Accepted: 23 Feb. 2021

ABSTRACT: On 21 October 2016, an earthquake with a magnitude of 6.6 (determined using the Japan Meteorological Agency's [JMA] seismic network) occurred in the center of Japan's Tottori Prefecture. In the city of Kurayoshi and in the towns of Yurihama and Hokuei, JMA seismic intensities of lower 6.0 were observed, and structural damage to housing was concentrated in a limited number of areas. This research conducted microtremor observations around damaged areas and used previous studies to estimate subsurface structures and ground motion characteristics. Low-velocity layers with an S-wave velocity of between 80 and 200 m/s were estimated at all observation sites and a tendency is present for the thickness to increase towards the coastal plains and decrease inland. In an evaluation of the relationship between ground motion characteristics and earthquake damage, researchers found that the occurrence of damage correlated to significant changes in layer thickness. Researchers believed that the damage correlates to the 2-D or 3-D effects of subsurface structures.

Keywords: Microtremor observation, Seismic observation, Subsurface structure, the 2016 central Tottori prefecture Earthquake

1. INTRODUCTION

An earthquake with a magnitude of 6.6 (according to the Japan Meteorological Agency's [JMA] seismic network) occurred in central Tottori Prefecture, Japan, on 21 October 2016. As Fig. 1 reveals, JMA seismic intensities of lower 6 were recorded in the city of Kurayoshi and in the towns of Yurihama and Hokuei [1]. In Hokuei, the damage to housing was concentrated in the town's flat areas, while in Yurihama, most damage occurred in the area at the mountain's edge [2,3]. This study suggests that the damage could be attributed to site amplification due to subsurface structures.

The earthquake's mainshock and its subsequent aftershocks were observed by NIED's K-NET and KiK-net strong motion seismograph networks, and at local government observation sites in Tottori Prefecture and at temporary sites at Tottori University. The analysis of those strong motion records suggests that the observed differences in site amplifications could be due to variations in subsurface structures. Furthermore, nonlinear soil responses due to strong ground motions were suspected at the Ryuto (TGAR) and Hisadome (YRAR) observation sites in the town of Yurihama and at the Hashita (HJA) site in Hokuei [3].

Data obtained from strong motion waveforms informed an estimation of the earthquake's source rupture process. Kubo et al. [4] show that the source model contains two major slip regions; in the first, the maximum slip extends from the hypocenter to the shallower area, while in the second, smaller slips are located NNW of the hypocenter.

A detailed understanding of the subsurface structure and ground motion characteristics is required to enable an evaluation of strong ground motions, nonlinear soil responses and the relationship between ground motion and damage. This study conducted microtremor observations around the strong motion observation sites and the earthquake-affected areas and estimated the subsurface structures and ground motion characteristics. The aftershock records were used to inform estimations of the deeper ground structures.

2. OBSERVATION

2.1 Damage to Housing and Previous Study of The Target Area

The mainshock of the 2016 earthquake caused damage that was concentrated in areas within the flatlands of the town of Hokuei and around the mountainside in the town of Yurihama. Figure 1 shows the affected areas; damage to roof tiles was initially determined based on blue sheet coverage identified from satellite images [5] and was confirmed by site visits and interviews. This study deems the damaged housing area to extend to a radius

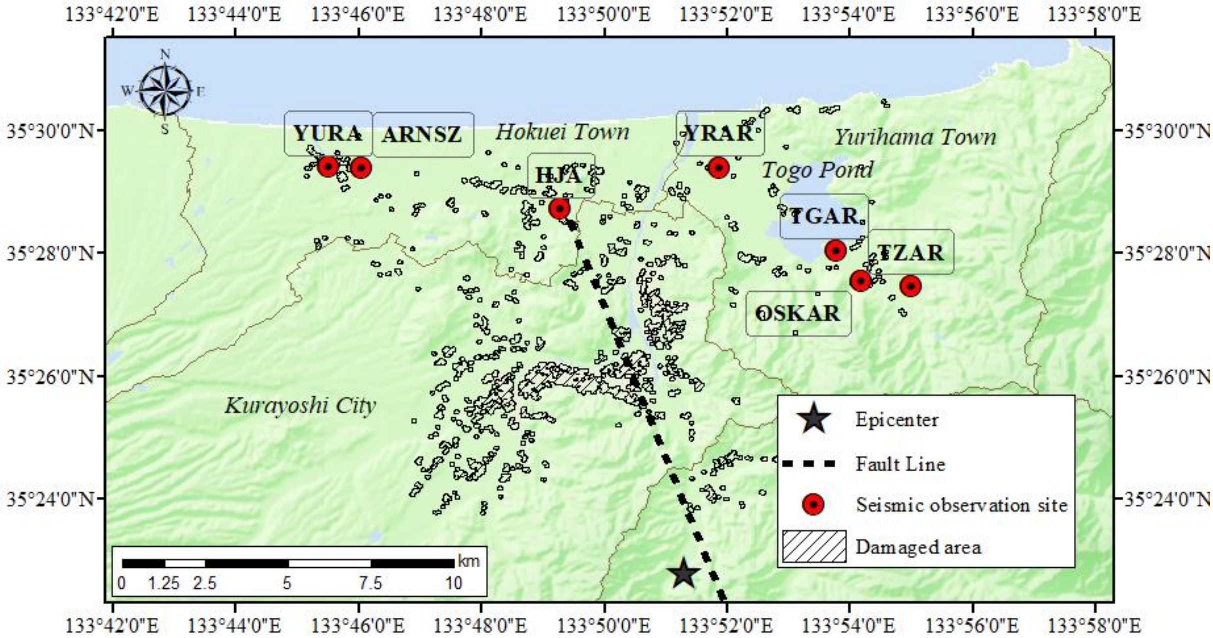

Fig.1 Epicenter and fault line [1], damaged area and seismic observation sites

of 50 m from the affected houses.

According to the previous studies [3,6], the predominant periods of the microtremors in Yurihama and Hokuei were between about 0.5 and 2.0 s and between 0.8 and 1.5 s, respectively. This study considers that these periods correspond to the thickness of soft layers with S-wave velocities below 400 m/s.

2.2 Summary of Observation

Single-point observations were conducted mainly in residential areas and strong motion observation sites at 294 locations in the town of Yurihama and at 162 sites in the town of Hokuei. Data were recorded using a JU410 three-component accelerometer with a 24-bit recorder at intervals of 50 m in areas of concentrated roof-tile damage. A wave amplification factor of 100, a sampling frequency of 100 or 200 Hz, and a recording time between 10–15 minutes were used.

As shown in Fig. 2, the study conducted array observations at four strong motion observation sites (YRAR, TGAR, HJA, and YURA) and three temporary aftershock observation sites (Oshikadani [OSK], Takatsuji [TZAR], and ARNSZ). The measurements were obtained using four JU410s synchronized by GPS clocks. One seismometer was placed at the center of a circle, and the other three were positioned around the circumference to form an equilateral triangle. A 200-Hz sampling frequency was used, the amplification factor was identical to that of the single-point observation, and the recording duration was around 15 minutes. According to the observation site, to evaluate the S-wave velocity structures of Quaternary sediments, the radius of the array was established between 0.6 to 30 m.

Aftershock observations were recorded at the OSK and TZAR sites, where major damage to roof tiles occurred. The OSK observation site was in operation between 24 July 2017 and 2 July 2018, while the TZAR site has been operating continually since 20 October 2015. A CV-374A sensor-integrated recorder was used for the observation at a sampling frequency of 100 Hz. The seismometers were installed indoors on solid bases where power was available, such as at the entrances to buildings.

3. ANALYSIS

3.1 Microtremor Records

Fourier spectra were calculated from a single-point observation record and were smoothed using a log window with a coefficient of 20 [7]. Average spectra were determined from at least 10 stable sections of 20.48 s. Horizontal to vertical (H/V) spectral ratios were calculated from the Fourier spectra, and the predominant periods were visually estimated. Many H/Vs were identified as unimodal with a single distinct peak. In cases where multiple peaks were observed in some areas, e.g. on mountainsides, the main areas were estimated with respect to continuity with adjacent unimodal sites. The entire predominant period distribution in the prefecture of central Tottori is detailed in Fig. 2.

To unify the velocity structure of the lowermost surface, an analysis of the array observations, including the re-analysis of past research data, was conducted [3,6], in accordance with the following procedure: the phase velocity dispersion curves of the array observation records were estimated based on the

CCA method [9]. Using the open analysis tool [8], at least five sections were selected by automatic extraction using the root mean square values of microtremor recordings with 10.24-s segments. Then, the power spectra within those sections were smoothed with a 0.3-Hz bandwidth Parzen window, and the average was obtained. Finally, the phase velocity dispersion curves were determined, and those obtained at each radius were integrated at each observation site, with respect to their continuity.

Both these curves and the microtremor H/Vs obtained from single-point microtremor recordings at the center of the array were used to inform the estimation of subsurface structure models from forward modeling based on the fundamental mode of Rayleigh waves. S-wave velocities were determined with reference both to previous studies [3,6] and borehole data surrounding the site [10]. Then, modeling was performed by modifying the thicknesses of the layers. The densities were established according to previous studies, and P-wave velocities were established based on the S-wave velocities [11]. The resulting subsurface structure model is presented in Table 1.

3.2 Aftershock Records

To ensure analytical consistency, the evaluation of aftershock records involved the use of data from both previous research [3,6] and from more recent observations. The analysis followed this procedure: time windows of 10.24 s with cosine tapers of 5% at both ends were applied from the arrival of the S-wave. The duration of the analysis record was extended to 20.48 s with the addition of zero data, and the Fourier spectrum was calculated and smoothed with a 0.2-Hz bandwidth Parzen window. The H/V spectral ratio (strong ground motion H/V) was evaluated based on the Fourier spectrum of each component. To obtain the H/V values at each site, around 10 aftershocks were analyzed and averaged.

Models of the subsurface structure were first estimated by forward modeling; the model was adjusted by comparing the observed and theoretical H/Vs based on the diffuse wave field theory [12] of strong ground motion H/Vs. To estimate shallow structures, the initial model employed the array observation models described above, while deep structures were assumed from previous research [6]. The final structure model was estimated from an inversion analysis by a hybrid heuristic search method [13] with a genetic algorithm (GA) and simulated annealing (SA). The damping constant, h, was assumed to be 0.03 for S-wave velocities of 100 m/s or less, 0.02 for velocities of 100 to 400 m/s, and 0.01 for those of 400 m/s or more. In this study, it was used the inversion code created by Yasui et al. [14].

The additional inversion parameters were as follows: the GA involved 10 trials, 30 samples, and 300 generations; the crossover probability was 0.7, the mutation probability was 0.01, and both dynamic mutation and elite selections were considered. For the SA, the temperature drop function was provided by Eq. (1), the coefficients were a = 0.5 and c = 1.0, the initial temperature was T0 = 100, and 10 temperature

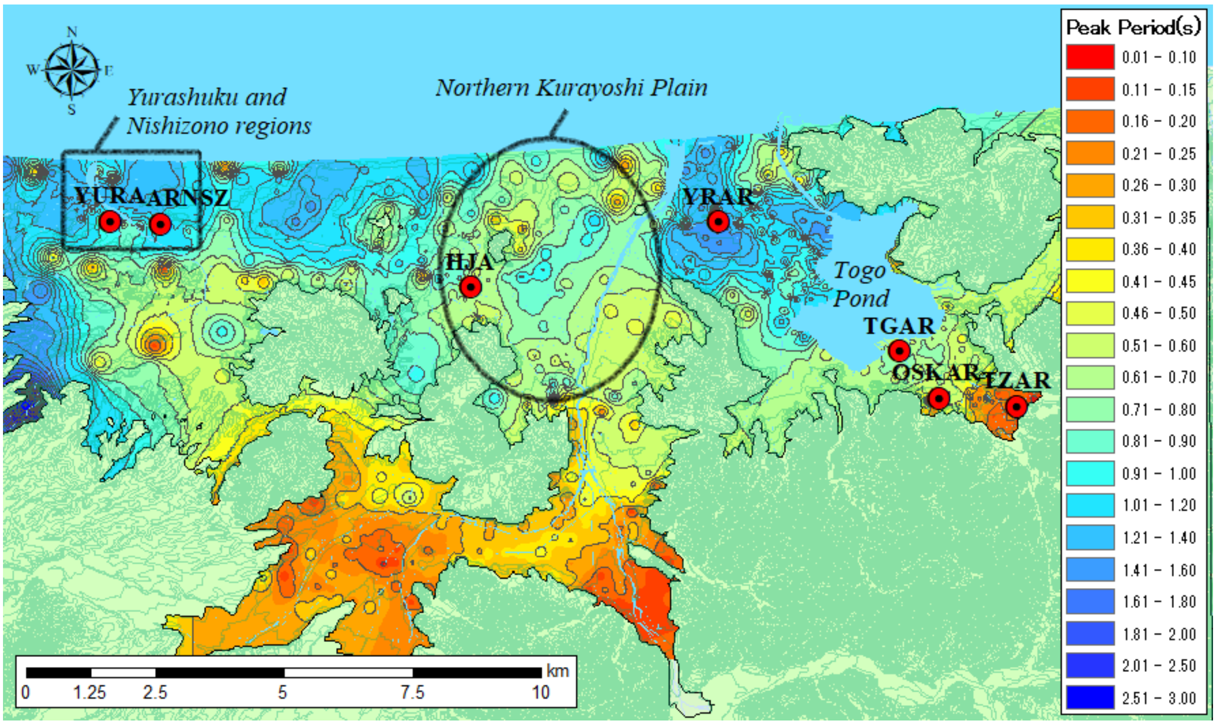

Fig.2 Predominant period distribution map in the prefecture of central Tottori

Table 1 Subsurface structures based on array observations

Yurihama Town

Site	Thickness (m)	ρ(t/m³)	Vp(m/s)	Vs(m/s)
YRAR (Hisadome)	33	1.6	1430	140
	75	1.8	1730	400
	100	2.1	2070	700
	∞	2.2	2620	1200
TGAR (Ryuto)	9	1.6	1390	90
	8	1.7	1510	200
	50	1.8	1730	400
	100	2.1	2070	700
	∞	2.2	2620	1200
OSKAR (Oshikadani)	8	1.6	1400	100
	3	1.7	1510	200
	30	1.8	1730	400
	100	2.1	2070	700
	∞	2.2	2620	1200
TZAR (Takatsuji)	4	1.6	1390	100
	4	1.7	1510	200
	100	2.1	2070	700
	∞	2.2	2620	1200

Hokuei Town

Site	Thickness (m)	ρ(t/m³)	Vp(m/s)	Vs(m/s)
HJA (Hashita)	9	1.6	1380	80
	5	1.7	1460	150
	10	1.8	1510	200
	12	1.9	1730	400
	∞	2.2	2620	1200
ARNSZ (Nishizono)	10	1.7	1430	130
	10	1.7	1510	200
	70	1.8	1730	400
	60	2.1	2070	700
	∞	2.2	2620	1200
YURA (Yurashuku)	11	1.7	1490	180
	65	1.8	1730	400
	80	2.1	2070	700
	∞	2.2	2620	1200

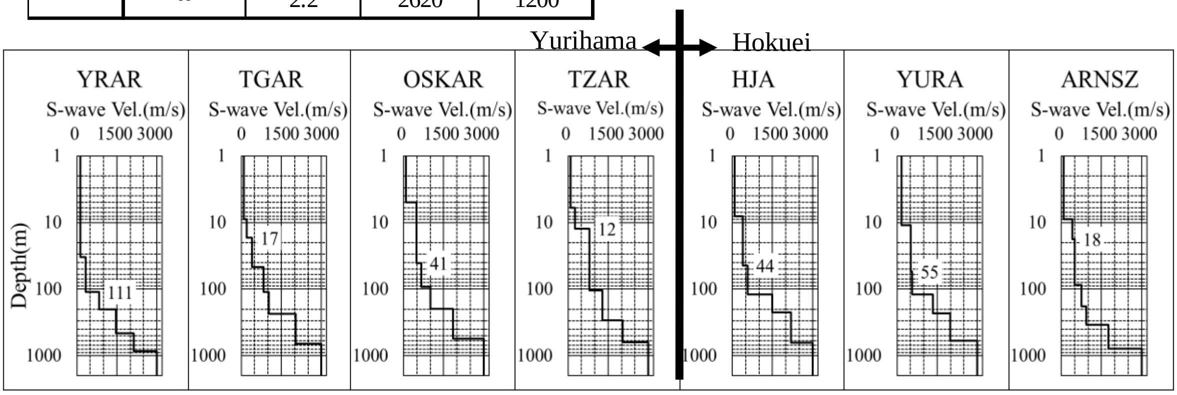

Fig.3 S-wave velocity structure column diagrams

updates occurred.

$$T = T_0 \exp\left(-ck^a\right) \quad (1)$$

The S-wave velocity and the thicknesses of the first and bottom layers were fixed, and the values of the other layers were searched within a range of ± 25% from the initial value. The search targets were the velocities and layer thicknesses of the S and P waves. The densities were established using an empirical formula [15] from the S-wave velocity. Figure 3 contains the resulting S-wave velocity column diagrams from the shallow to the deep layers.

4. DISCUSSIONS

4.1 Major Periods of The Horizontal to Vertical Spectral Ratios of Microtremors

Figure 2 shows that the predominant periods around the YRAR site were 0.8 to 1.6 s, while around the TGAR, OSKAR, and TZAR sites, they were between 0.4 and 0.8 s. Around the ARNSZ and YURA sites, the main periods were 1.0 to 1.6 s, while those at HJA in the N Kurayoshi Plain were between 0.4 and 1.0 s. Many single-peak microtremor H/Vs were observed on the N Kurayoshi Plain and around Togo Pond, and many multiple-peak H/Vs were recorded in the regions of Nishizono and Yurashuku (Fig. 4). It is likely that this distribution reflects variations in velocity structures in the surface layers.

4.2 Estimation of Subsurface Structures

Based on the borehole data from around the observation sites [9], the S-wave velocities of 100 m/s or less given in Table 1 are considered to have occurred in clay or silt layers, while an S-wave velocity of 200 m/s is considered to have occurred in a sand layer. It is evident from Table 1 that the soft layer with an S-wave velocity of between 80 and 200 m/s is between 6 and 33 m thick at each site; a tendency is present for the thickness to increase towards the coastal plains and decrease inland. Silt layers with S-wave velocities between 80 and 140 m/s in the surface layer were identified at the YRAR, TGAR, and HJA observation sites. Researchers suggested that the nonlinear responses reported in these areas were caused by dominant layers of silt.

Aftershock observation records informed the estimation of deeper subsurface structures in this study. In Fig. 3, the numbers indicate the depth from the surface layer to the engineering seismic base layer. The depth tends to be deeper towards the coastal plain in the subsurface structure model, which is consistent with the tendency for the predominant periods to elongate towards the plains. The thicknesses of the deeper subsurface structures with S-wave velocities exceeding 700 m/s differ between the towns of Yurihama and Hokuei.

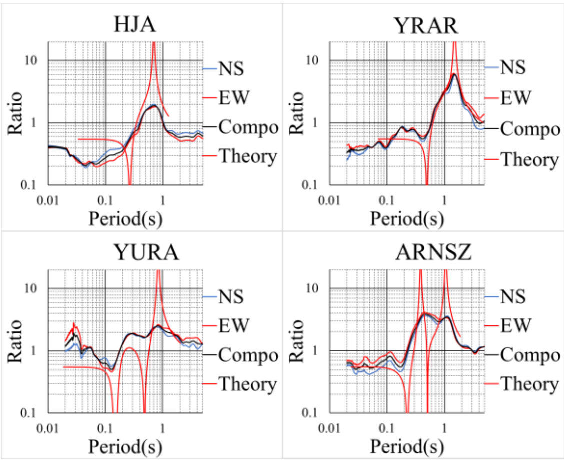

Fig.4 Microtremor horizontal to vertical spectral ratios at the center of the array observation sites

4.3 Consideration of Housing Damage

At each site, the amplification was evaluated using AVS30 and ARV ground amplification indicators [16]. Equation (2) was used to calculate the ARV. The average S-wave velocity at underground depths down to 30 m is represented by the AVS30 indicator, and Table 2 presents the AVS30 and ARV values at each site. At the YRAR and HJA sites, where major structural damage was not observed, the ARV value is around 2.5, while at the OSKAR and ARNSZ sites, which suffered widespread damage, ARV values of around 2.0 are evident. However, no clear relationship is identified between structural damage and ARV.

$$logARV = 1.83 - 0.66logAVS30 \qquad (2)$$

Table 2 AVS30 and ARV at array sites

Yurihama	YRAR	TGAR	OSKAR	TZAR
AVS30	140	174	220	328
ARV	2.59	2.25	1.98	1.48

Hokuei	HJA	ARNSZ	YURA
AVS30	142	197	276
ARV	2.56	2.07	1.65

Surface layer thicknesses were estimated, and specific changes were examined in the areas of concentrated structural damage in the Nishizono and Yurashuku regions. Next, the S-wave velocities and the predominant periods (Tp) were used to estimate the layer thicknesses (H) from Eq. (3). In both areas, a short predominant period, Tp1, and a long predominant period, Tp2, were estimated, and the layer thicknesses were estimated using the peaks from Eq. (3).

$$H_i = \frac{V_S \cdot T_{pi}}{4} \qquad (3)$$

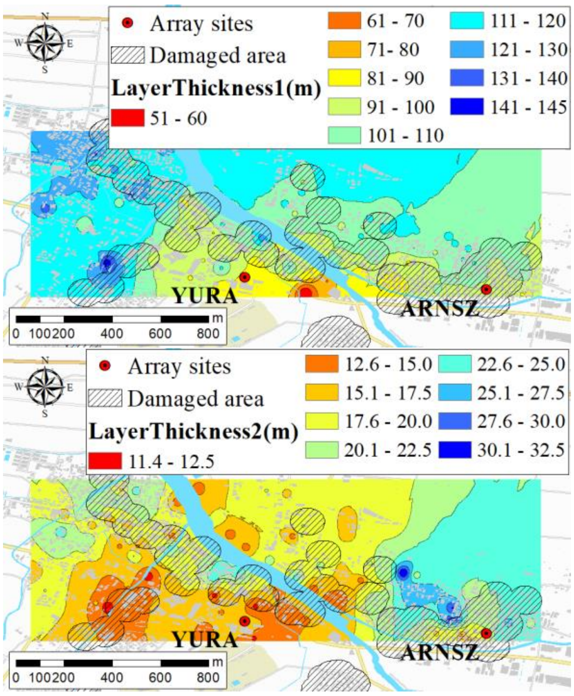

Fig.5 Layer thicknesses in the Nishizono and Yurashuku regions (upper map: Tp1, lower map: Tp2)

It is evident from Fig. 5 that the layer thicknesses from Tp1 are deeper from the S to the NW and the layer thicknesses from Tp2 are deep in only limited areas. A comparison between the affected areas and the layer thicknesses reveals an overlap along the boundary where the layer thickness of Tp2 changes. This intersection indicates the impacts of 2-D or 3-D shapes on structural damage within the engineering seismic base.

5. CONCLUSION

This research investigated microtremor and earthquake observations in the areas damaged by the 2016 earthquake in the Japanese prefecture of central Tottori. The relationship between subsurface structures, ground motion characteristics, and earthquake damage was considered via estimations and evaluations. Consequently, the following findings are noted.

A tendency is evident for H/Vs obtained from a single-point microtremor observation to possess longer predominant periods in coastal plains than in inland areas.

Phase velocity dispersion curves were obtained from microtremor array observation data, and they were used to inform the estimates of S-wave velocity structures. At the YRAR, TGAR, and HJA observation sites, where nonlinear responses were observed, the surface layers were found to contain low-velocity silt layers; it is highly likely that these layers are related to the nonlinear responses at the study locations.

The aftershock observation records informed the estimations of deeper subsurface structures. Consequently, variations were identified between the depths of the deeper subsurface structures, with S-wave velocities exceeding 700 m/s in the towns of Yurihama and Hokuei.

A comparison between the observed structural damage and the ground amplification indices estimated from this study's models was found to be weak in relevance. However, from the layer thicknesses estimated from the predominant periods and the surface S-wave velocities, researchers discovered that damage occurred at those sites where the layer thickness changed dramatically. Therefore, researchers suspected that the earthquake damage resulted from the 2-D or 3-D effects of irregular subsurface structures. This finding will be further explored in future research.

6. ACKNOWLEDGMENTS

This study used the code developed by Dr Yuzuru Yasui for the inversion analysis. Mr Ichihashi, a member of the local government volunteer fire department, and Mr Yamamoto, a technical staff member of the Faculty of Engineering at Tottori University, assisted in establishing observation sites at Oshikadani and Takatsuji as well as collecting data and reporting local damage. The authors would like to thank Enago (www.enago.jp) for the English language review. We appreciate to everybody who supported our study.

7. REFERENCES

[1] Japan Meteorological Agency, Evaluation of the earthquake on October 21, 2016 in central Tottori Prefecture,<https://www.static.jishin.go.jp/resource/monthly/2016/20161021_tottori.pdf>,[Viewed on 11 June 2020].

[2] Kagawa T., 2016 Central Tottori Earthquake (M6.6), Earthquake Journal, No.63, 2017, pp.14-22. (in Japanese)

[3] Kagawa T., Noguchi T., Yoshida S. and Yamamoto S., Effect of the surface geology on strong ground motions due to the 2016 Central Tottori Earthquake, Japan, Earth, Planets and Space, 69:106 DOI 10.1186/s40623-017-0689-0, 2017.

[4] Kubo H., Suzuki W., Aoi S. and Sekiguchi H., Source rupture process of the 2016 central Tottori, Japan, earthquake (MJMA 6.6) inferred from strong motion waveforms, Earth, Planets and Space 69:127 DOI 10.1186/s40623-017-0714-3, 2017.

[5] Honda Y., Mochizuki K., Shimomura H. and Monma N., Automatic extraction of blue sheet-covered housing from satellite images of 2016 Central Tottori Earthquake, Japan Society for Disaster Information Studies, Proceedings of the 19th conference, 2017, pp.244-245. (in Japanese)

[6] Noguchi T., Nishikawa H., Yoshida S. and Kagawa T., Estimation of subsurface structure and characteristics of ground vibration based on microtremor and seismic observation in the central Tottori Prefecture, Japan, Journal of Japan Association for Earthquake Engineering, Vol. 19, Issue 6, 2019, pp 258-271. (in Japanese with English abstract)

[7] Konno K. and Ohmachi T., A smoothing function suitable for estimation of amplification factor of the surface ground from microtremor and its application, Transactions of the Japan Society of Civil Engineers, No525/I-33, 1995, pp247-259. (in Japanese with English abstract)

[8] Cho I., Tada T. and Shinozaki Y., Possibility of microtremor array opened up by general theory: Release of analysis tool BIDO, Seismological Society of Japan Fall Meeting in 2009. (in Japanese)

[9] Cho I., Tada T. and Shinozaki Y., Centerless circular array method: Inferring phase velocities of Rayleigh waves in broad wavelength ranges using microtremor records, J. Geophys. Res., 111, B09315, 2006.

[10] National Research Institute for Earth Science and DisasterResilience:GeoStation,<https://www.geostn.bosai.go.jp/>, [Viewed on 9 October 2019].
[11] Kitsunezaki C., Goto N., Kobayashi Y., Ikawa, T. Horike M., Saito T., Kurota T., Yamane K. and Okuzumi K., Estimation of P- and S- wave velocities in deep soil deposits for evaluating ground vibrations in earthquake, Natural disaster science, 9-3, 1-17, 1990. (in Japanese with English abstract)
[12] Kawase H. Sanchez-Seama F.J. and Matsushima S., The optimal use of horizontal-to-vertiacal spectral ratios of earthquake motions for plane waves, Bull. Seism. Soc. Am. Vol.101, No.5, 2011, pp.2001-2014.
[13] Yamanaka H., Inversion of surface-wave phase velocity using hybrid heuristic search method, Geophysical Exploration, Vol. 60, Issue 3, 2007, pp-265-275. (in Japanese with English abstract).
[14] Yasui Y., Nishikawa H., Maeda T., Cho I., Kojima K., Koketsu K. and Miyajima M., Applicability of an inversion of earthquake H/V spectral ratios for soil structures – a case study using records in Fukui Prefecture, JSCE Journal of Earthquake Engineering, Vol.70, Issue 4, 2014, pp.628-643. (in Japanese with English abstract)
[15] Ota T., Emori K. and Kasai Y., Building foundation earthquake resistance / vibration / control, Kyoritsu Shuppan, 2001, pp-339.
[16] Midorikawa S., Matsuoka M. and Sakugawa K., Site Effect of Strong- Motion Records Observed during the 1987-Chiba-kentoho-oki, Japan Earthq. Eng. Sympo, Vol.3, 1994, pp.85-90.